Topical Developments in High-Field Dynamic Nuclear Polarization

Vladimir K. Michaelis[1,2‡], Ta-Chung Ong[1,2‡], Matthew K. Kiesewetter[1], Derik K. Frantz[1], Joseph J. Walish[1], Enrico Ravera[3], Claudio Luchinat[3], Timothy M. Swager[1] and Robert G. Griffin[1,2]*

[1]Department of Chemistry and [2]Francis Bitter Magnet Laboratory, Massachusetts Institute of Technology, Cambridge, Massachusetts, 02139, USA

[3]Department of Chemistry "Ugo Schiff" and Magnetic Resonance Center (CERM) University of Florence, 50019 Sesto Fiorentino (FI), Italy

*Corresponding author: rgg@mit.edu

Keywords: DNP, NMR, cross-effect, radicals, polarizing agent, cryoprotection

Abstract:

We report our recent efforts directed at improving high-field DNP experiments. We investigated a series of thiourea nitroxide radicals and the associated DNP enhancements ranging from $\varepsilon = 25$ to 82 that demonstrate the impact of molecular structure on performance. We directly polarized low-gamma nuclei including ^{13}C, ^{2}H, and ^{17}O using trityl via the cross effect. We discuss a variety of sample preparation techniques for DNP with emphasis on the benefit of methods that do not use a glass-forming cryoprotecting matrix. Lastly, we describe a corrugated waveguide for use in a 700 MHz / 460 GHz DNP system that improves microwave delivery and increases enhancement up to 50%.

Introduction

During the past two decades, magic-angle spinning (MAS) NMR spectroscopy has emerged as an excellent analytical method to determine atomic-resolution structures in various chemical systems including pharmaceuticals,[1-3] membrane proteins,[4-8] and amyloid fibrils.[9-13] Unfortunately, NMR sensitivity is inherently low and consequently many experiments require long acquisition times to achieve adequate signal-to-noise. A promising route to increase NMR sensitivity is via dynamic nuclear polarization (DNP), which seeks to polarize nuclear spins using electron polarization transferred via microwave irradiation of electron-nuclear transitions. In particular, the method has been shown to provide increases in polarization upwards of 2 to 3 orders of magnitude.[14-20]

Dynamic nuclear polarization was initially demonstrated in the 1950s at low magnetic fields. Following the groundbreaking work of Overhauser,[21] Carver, and Slichter,[22] various polarization-transfer mechanisms were studied in the 1960s and 1970s including the solid effect (SE),[23-25] the cross effect (CE),[26-30] and thermal mixing (TM).[18,31-33] However, the theoretical understanding of the DNP mechanisms suggested limited applicability at magnetic fields beyond 1 T. This was followed by a brief exploration of applications of DNP to polymers at low fields (1.4 T) by Wind *et al.*[18], Schaefer and co-workers.[34,35] Moreover, DNP experiments at higher fields (≥ 5T) was hindered by the lack of stable, high-power microwave devices operating at the necessary high frequencies (e.g., 100 to 600 GHz) and also by the absence of low-temperature, high-resolution MAS NMR probes that offer both effective microwave coupling as well as the required sample cooling. Together these barriers prevented DNP from being widely applicable in the decades following its discovery. In the early 1990's, our laboratory introduced high frequency gyrotron (a.k.a. cyclotron resonance maser) sources to magnetic resonance and DNP in particular since they can reliably provide high-frequency microwaves.[36] They have now made high-field DNP viable for many applications. Combined with the improved resolution offered with higher-field MAS experiments, DNP can now be used to investigate many chemically challenging systems and areas of NMR spectroscopy including biological solids[37-41], surface chemistry[42], and systems involving difficult NMR-active nuclei (e.g., low natural abundance, low gamma and / or quadrupolar).[43-49]

The DNP mechanism involves microwave irradiation of the EPR transitions of a paramagnetic polarizing agent that transfers the large spin polarization of electrons to nearby nuclei. In order to accomplish this at contemporary NMR fields (i.e., 200 to 1000 MHz), three criteria must be met: i.) a stable high-frequency microwave source (≥ 10^2 GHz), ii.) a reliable cryogenic MAS probe with adequate microwave waveguide delivery, and iii.) a suitable

polarizing agent for the sample under study. The first criterion was met by the aforementioned gyrotrons, which are fast wave devices that can deliver the appropriate frequency range for stimulation of the EPR transitions at high fields, and they can be operated stably and continuously over an extended period of time (i.e., weeks to months).[50] Second, to date DNP is optimally performed at cryogenic temperatures to decrease electron and nuclear relaxation rates in order to increase the obtainable non-Boltzmann polarization. To achieve the desired temperature (80-100 K) typically requires a specially designed heat exchanger / dewar system,[51] vacuum-jacketed gas-transfer lines, and optional pre-chillers.[52,53] The complexity of this instrumentation is further compounded by the need for MAS in order to obtain high resolution spectra, meaning that carefully designed and constructed multichannel (e.g., $^{1}H/^{13}C/^{15}N/e^{-}$) low-temperature MAS NMR probes are essential.[54] The third requirement is the availability of paramagnetic species (polarization agents) that is the polarization source for various chemical systems. The polarizing agent can be exogenous or endogenous and most often comes in the form of a free radical. It should be compatible with the chemical system (e.g., non-reactive), able to yield large DNP enhancements, and chemically robust. Depending on the application, the radicals and experimental conditions can be developed to optimize a specific DNP mechanism[55,56] such as SE or CE.

Over the past two decades, development of high-field DNP has focused primarily on using the CE mechanism, since the typical SE enhancements had been considerably lower.[57] Below we make mention of both the SE and CE mechanism as recent results have shown that the SE may be useful for polarization using transition-metal based polarizing agents[58] and recently been observed to provide significant enhancements ~100.[59,60] Furthermore, with the continued development of equipment producing increased microwave field strengths, the enhancements and sensitivity may match those of CE.[61] The dominant polarization transfer process (SE or CE)

depends on the NMR-active nuclei being polarized and also the EPR characteristics of the specific polarizing agent. Particularly, the relative magnitudes of the electron homogeneous (δ) and inhomogeneous (Δ) linewidths, and the nuclear Larmor frequency (ω_{0I}) are the most important factors to determine the dominant polarization mechanism.

The SE mechanism, shown in Scheme 1, is a two-spin process which is dominant when $\omega_{0I} > \delta, \Delta$ and microwave irradiation is applied at the electron-nuclear zero- or double-quantum transition.[24,25,59,60] This matching condition is given by:

$$\omega_{\mathrm{mw}} = \omega_{0S} \pm \omega_{0I} \qquad (1)$$

where ω_{0S} is the electron Larmor frequency and ω_{mw} is the microwave frequency. For SE, since the microwave frequency required must match the condition given in Eq. (1), a polarizing agent with a narrow EPR spectrum is typically used, with an electron T_{1S} that is optimized to allow efficient polarization of nearby nuclei without introducing large signal quenching.

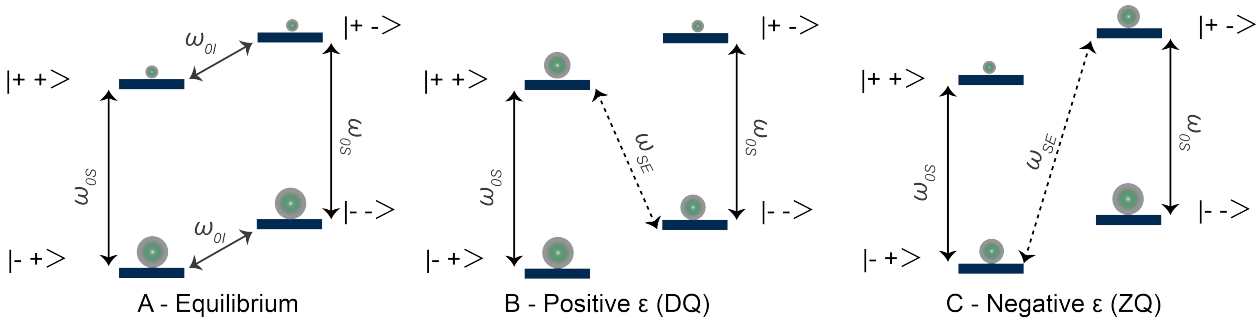

Scheme 1: Spin population distribution for a two-spin (1 electron and 1 nucleus) system at thermal equilibrium (A). SE conditions for the positive, $\omega_{0S} - \omega_{0I}$ (B) and negative enhancement, $\omega_{0S} + \omega_{0I}$ (C).

The CE mechanism may be described as a three-spin flip-flop-flip process between two electrons and a nucleus, which is dominant when $\Delta > \omega_{0I} > \delta$. In order to achieve maximum efficiency, the difference between the two electron Larmor frequencies must be near the nuclear Larmor frequency.[26,28,62,63]

$$\omega_{0I} = \omega_{0S_2} - \omega_{0S_1} \qquad (2)$$

For CE[64], a radical with a broad EPR linewidth, particularly a nitroxide based radical, is often used to satisfy the condition provided in Eq. (2). CE is often the choice for high-field DNP experiments due to this mechanism being based on allowable transitions unlike the SE. Scheme 2 shows the energy level diagram for the CE mechanism.

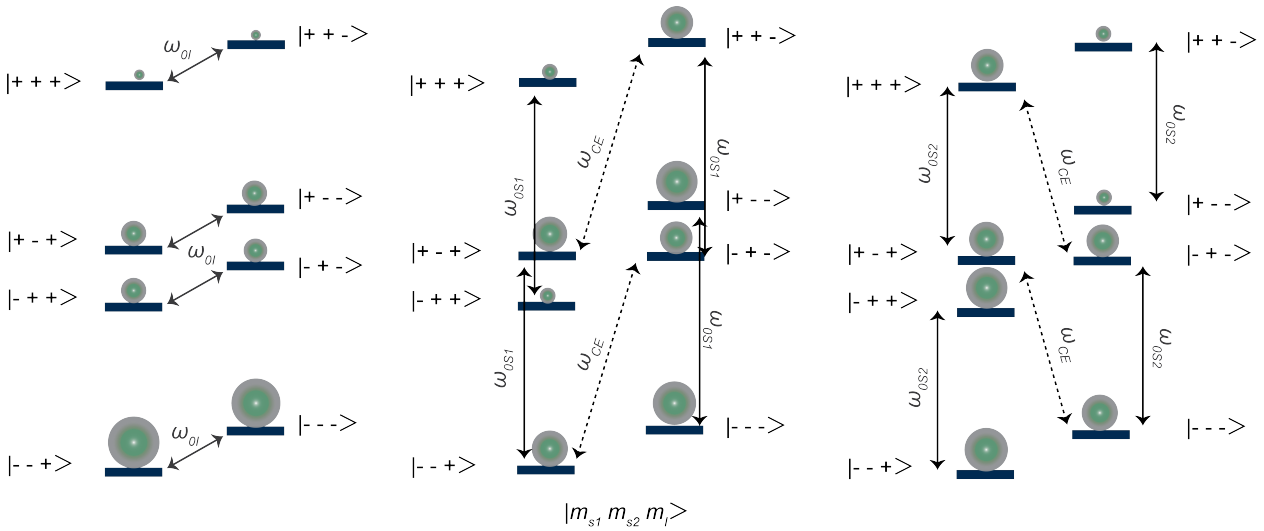

Scheme 2: Spin population distribution for a three-spin (2 electrons and 1 nucleus) system at thermal equilibrium with the NMR transitions marked (A). The CE condition for the negative (B) and positive (C) enhancement. Microwave saturation of the electron transition (ω_{0S1} or ω_{0S2}) leads to a three-spin flip-flop-flip process that distributes the population (ω_{CE}), thus increasing the net nuclear polarization.

The descriptions for the CE and the SE DNP mechanism, *vide supra,* do not incorporate sample rotation. That is, the effects of MAS on modulating energy levels that create level crossings and impact polarization transfer. Recently, Thurber and Tycko[65] and Mentink-Vigier *et al.*[66] discussed the CE mechanism in MAS, while showed experimental MAS DNP NMR data on the SH3 protein and described theoretical models of the effect MAS has on both the CE and the SE mechanism.

In this paper, we provide a brief overview of recent developments in high-field DNP at the Francis Bitter Magnet Lab at MIT, including polarizing agents, sample preparation methods, and improvements to the 700 MHz / 460 GHz DNP spectrometer.

i. Development of CE Biradicals

Nitroxide monoradicals (e.g., TEMPOL) were popular in early high-field DNP experiments. They are suited for CE DNP of ^{1}H because the breadth of the EPR spectrum is of the order of ~600 MHz.[67] They are also low-cost, commercially available, highly water-soluble, and offer reasonable DNP enhancements between ε =20 to 50.[36,68] For these monoradicals, a concentration of up to 40 mM usually provides the best signal enhancements. However, at these elevated electron concentrations, paramagnetic relaxation strongly competes with DNP enhancement and only provides moderate electron-electron dipolar couplings between 0.2 to 1.2 MHz. Increasing the concentration of radical further is unsuitable for high-resolution NMR work because of line broadening and signal quenching effects at these higher radical concentrations.

To improve the CE efficiency, biradicals were introduced for DNP in order to improve the electron-electron dipolar coupling critical to CE DNP while lowering the overall radical concentration to minimize paramagnetic effects (i.e., signal quenching and broadening). By tethering two TEMPO monoradicals, one such biradical, TOTAPOL,[69] has an effective electron – electron coupling of ~ 26 MHz, is water-soluble, and provides greater ^{1}H enhancements than TEMPO based monoradicals by nearly four-fold at 5 T as shown in Figure 1. The discovery of TOTAPOL as a polarization agent and the then-unprecedented signal enhancements it produced belies the extreme sensitivity that molecular perturbations affect upon CE efficiency. Tethering nitroxide radicals introduces several parameters that can be optimized, and synthetic organic

chemistry is the primary tool of modulating dipolar coupling (i.e. inter-electron distance), g-tensor orientation, water solubility, and relaxation behaviors. All of these factors impact the resulting DNP signal enhancement. The large synthetic opportunity has led us and others to pursue new generations of biradicals in order to achieve even greater DNP enhancements.[70-73]

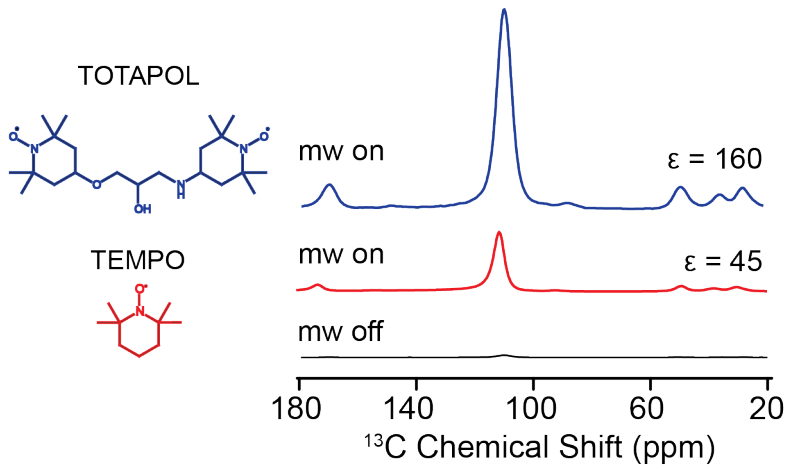

Figure 1: $^{13}C\{^{1}H\}$ cross-polarization of ^{13}C-urea in a 60/30/10 v/v d_8-glycerol/D_2O/H_2O with 20 mM TOTAPOL (top, ^{1}H DNP) and 40 mM TEMPO (bottom, ^{1}H DNP) acquired at 140 GHz / 212 MHz DNP NMR spectrometer with 8 W of microwave power, 4.5 kHz MAS, and 16 scans (on-signal) and 256 scans (off-signal).

Here we examine a series of biradicals that are structural variants of bT-thiourea to illustrate the impact of molecular structure upon DNP enhancement. The bT-thioureas were synthesized to improve aqueous solubility exhibited by bT-urea[64], but they have a lower enhancement as shown in Figure 2. The reason for this reduction in obtainable signal enhancement from bT-urea to bT-thiourea (bT-thio-3) may be due to a compression of the TEMPO moieties from the increased steric bulk stemming from the sulfur (as opposed to oxygen) in the thiourea, or alternatively it may be due to an undesirable gain in torsional mobility upon switching the urea group to a thiourea group. We observed a further loss of DNP enhancement

upon utilizing the bT-thionourethane (bT-thio-2) biradical. The increased conformational flexibility of the bT-thionourethane may be deleterious in that the only other conformation available to this molecule (versus BT-thiourea) features the oxygen-bound TEMPO moiety beneath the thionourethane linker. This would result in a reduced inter-electron distance similar to other highly-coupled biradicals.[64] Nevertheless, it should be noted that increasing conformational flexibility is not always deleterious. bT-thionocarbonate (bT-thio-1) is the most conformationally flexible structural variant studied, and it shows a larger enhancement than bT-thionourethane. The slightly preferred s-*trans* orientation of thionocarbonates is apparently more than enough to compensate for the modestly diminished inter-electron distance resulting from the shorter C-O (vs. C-N) bonds, therefore producing a DNP enhancement similar to that of bT-thiourea (BT-thio-3).

The study of the bT-thiourea-based radicals highlights the multi-dimensional problem of developing radicals for DNP. As the study continues, more effective radicals will be discovered for DNP application to different chemistry problems. For example, many biradicals currently are optimized for dissolution in cryoprotectants such as glycerol/water or DMSO/water for studying biological samples at cryogenic temperatures.[69,70] The glassing behavior of cryoprotectants disperses the radical homogeneously throughout the sample and allows uniform polarization. Amongst organic solids, some systems have meta-stable amorphous phases such as the anti-inflammatory drug indomethacin,[74,75] but they may not be miscible with existing biradicals such as TOTAPOL for effective DNP experiments. For this reason, we used the organic biradical bis-TEMPO terephthalate (bTtereph) for our DNP study on amorphous *ortho*-terphenyl and amorphous indomethacin.[76] We found that the biradical exhibits similar EPR and DNP profiles as TOTAPOL (Figure 3) and can be incorporated uniformly within amorphous *ortho*-terphenyl and indomethacin samples without needing other glassing agents.

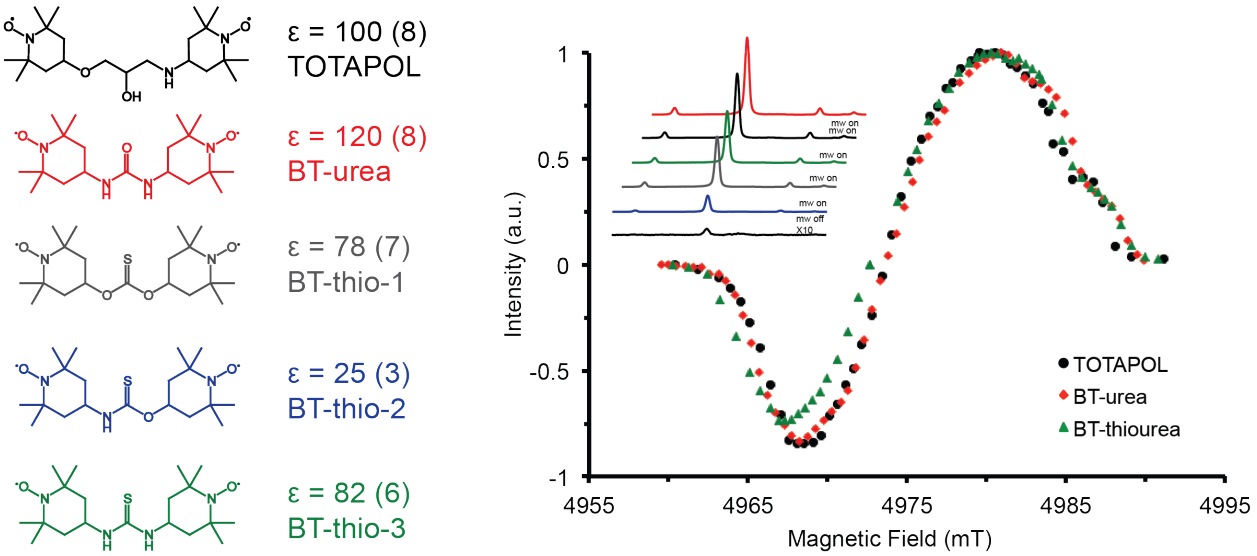

185

186 **Figure 2:** $^{13}C^{1}H$ cross-polarization spectra of ^{13}C-urea in DMSO/D_2O/H_2O (60:30:10, v/v) and 10 mM
187 biradical polarizing agent (20 mM electrons) acquired at 140 GHz / 212 MHz DNP NMR spectrometer with
188 8 W of microwave power. ^{1}H DNP enhancements were scaled with respect to TOTAPOL using three
189 thiourea variants. From top to bottom five radicals were studied including TOTAPOL (black), BT-urea (red),
190 BT-thio-1 (thionocarbonate, grey), BT-thio-2 (BT-thionourethane, blue) and BT-thio-3 (BT-thiourea, green).
191 The spectra inset are the on/off $^{13}C[^{1}H]$ CPMAS spectra scaled to the TOTAPOL enhancement in
192 DMSO/water mixture.

193

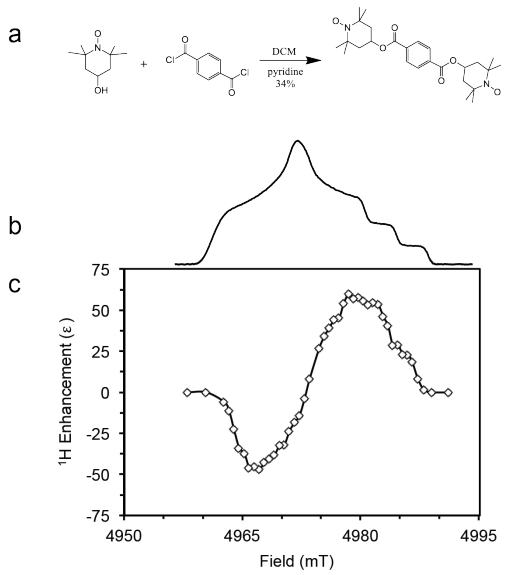

Figure 3: BT-Tereph synthetic process (a) and resulting 140 GHz EPR spectrum (b) and ^{1}H DNP field (c) profile of 10 mM bTtereph incorporated in 95% deuterated amorphous ortho-terphenyl.

More recently, a new truxene-based radical, TMT, was found to be persistent, having a half-life ($t_{1/2}$) of 5.8 h in a non-aqueous solution exposed to air.[77] EPR at 140 GHz shows a g-value very close to that of BDPA[78] and a linewidth of 40 MHz (Figure 4). The radical may be ideal for supporting the CE, either alone for low-γ nuclei such as ^{15}N, or as part of a biradical or radical mixture with Trityl OX063 or TEMPO.[57,79] Current work is aimed at increasing the radical's solubility in aqueous solvent mixtures suitable for DNP of biological samples and improving its stability under ambient conditions.

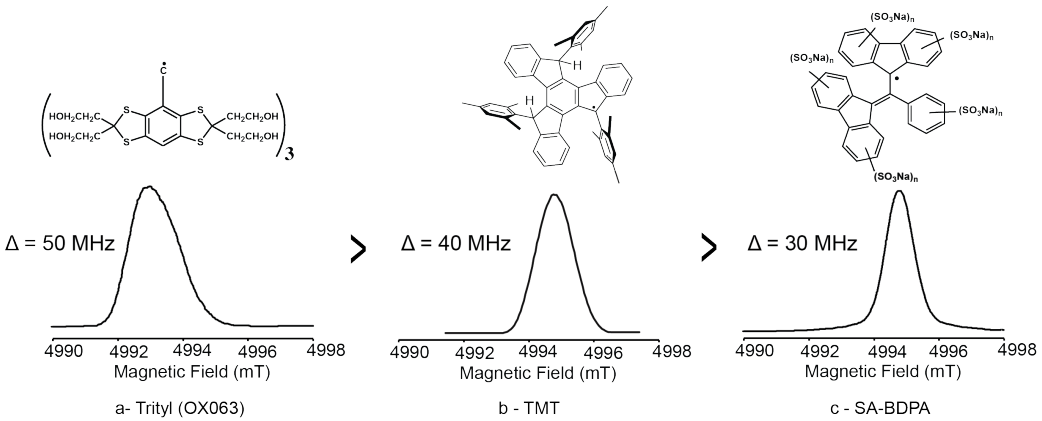

206

207 **Figure 4:** Chemical structures and 140 GHz EPR spectra of three narrow-line radicals: (a) Trityl, (b) TMT,
208 and (c) SA-BDPA.

209 *ii. Direct Polarization of Low-Gamma Nuclei using Trityl*

210 Currently, the conventional wisdom is that the most efficient electron-nuclear transfer
211 mechanism in the solid state is the CE. Consequently, many polarization agents are designed
212 from nitroxide based radicals due to their broad EPR profile easily satisfying the CE match
213 condition in Eq. (2) for ^{1}H. For many systems, polarizing ^{1}H by CE is an effective method
214 because ^{1}H typically have shorter relaxation times, which enables rapid signal averaging as well
215 as offers additional gains by means of cross-polarization to other low-gamma nuclei that are often
216 less abundant. However, direct polarization of low-gamma nuclei is also of interest considering
217 the theoretical maximum DNP enhancement is given by the ratio γ_e/γ_I. Focusing on the five most
218 common nuclei found in biological molecules, three of which are I=1/2 (i.e., ^{1}H, ^{13}C and ^{15}N)
219 while ^{2}H is I=1 and ^{17}O is I=5/2. With the exception of ^{1}H, these nuclei are low-gamma and low
220 natural abundance (Table 1). Moreover, the latter two nuclei are quadrupolar and consequently
221 experience additional line broadening brought about by the interaction between the intrinsic
222 electric quadrupole moment and the electric field gradient (EFG) generated by the surrounding
223 environment, thereby giving rise to quadrupolar coupling. This additional interaction negatively

impacts NMR sensitivity because the quadrupolar coupling constant covers a spectral range from tens of kHz up to a few MHz. With these factors in mind, DNP experiments that directly polarize low-gamma and/or quadrupolar nuclei can potentially be useful and open new possibilities for high field DNP.

For the direct polarization experiments, we can utilize narrow-line radicals that satisfy the CE match condition of low-gamma nuclei to provide effective electron polarization transfer. The water-soluble narrow-line monoradical trityl[80,81] with its EPR spectrum is depicted in Figure 4. The EPR spectrum is considerably narrower than that of the common nitroxide based radicals, with a linewidth of approximately 50 MHz at 5 T.[48,79,82] This narrow profile creates the possibility for both SE and/or CE mechanism to contribute to the DNP enhancement depending on the targeted nucleus. In order to determine the effectiveness of trityl on three low-gamma nuclei (i.e., ^{13}C, ^{2}H, and ^{17}O), a series of DNP experiments were attempted, followed by the characterization of the mechanisms with assistance from the DNP field profiles (Figure 5).

Table 1: Physical properties for select biologically relevant NMR nuclei.

NMR Active Isotope	N.A. (%)	Magnetogyric Ratio (MHz / T)	Sensitivity relative to ^{1}H	Theoretical ε_{max}
^{1}H	99.99	42.57	1	658
^{13}C	1.07	10.71	1.7×10^{-4}	2616
^{2}H	0.01	6.53	1.11×10^{-6}	4291
^{17}O	0.037	5.77	1.11×10^{-5}	4857

For direct polarization of ^{13}C, we obtained an enhancement of 480 (Figure 6a) using trityl, which is nearly 180% larger than using TOTAPOL.[79,83] Examining more closely at the positive and negative maxima of the DNP profile, we can see there is a clear asymmetry (i.e., -380 vs. 480) present. However, unlike the ^{1}H field profile of trityl[59] there is no feature in the center of the profile between the two maxima. This suggests that CE polarization mechanism is making some contribution to the DNP mechanism. Nevertheless, the nuclear Larmor frequency of ^{13}C is slightly larger than the breadth of the trityl EPR spectrum at 5 T, and therefore by definition the SE must be considered. Looking at the positive and negative maxima of the ^{13}C DNP field profile, the positions are in remarkably good agreement (Figure 5, blue dotted lines) with those predicted for the SE mechanism, suggesting a significant contribution.

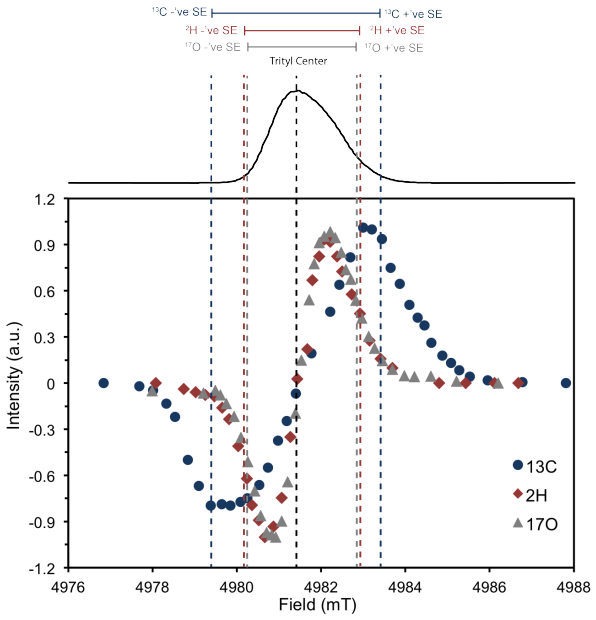

Figure 5: Direct polarization of ^{13}C (circle, blue), ^{2}H (diamond, red) and ^{17}O (triangle, grey) field profiles acquired at 5 T using 40 mM Trityl radical. 140 GHz EPR spectrum of trityl (black, top) with the appropriate SE matching conditions illustrated with the corresponding colored dashed lines.

The nuclear Larmor frequencies of ^{2}H and ^{17}O are separated by only ~ 4 MHz at 5 T and appear to behave similarly as the field profiles are nearly overlapping. Although the electron inhomogeneous linewidth of the trityl radical is small, it is still large enough to satisfy the CE match condition for both nuclei. Both field profiles do not exhibit resolved features at frequencies corresponding to $\omega_{0S} \pm \omega_{0I}$ (Figure 5, red and grey lines), which assures that the CE mechanism is dominant for both ^{2}H and ^{17}O. For static DNP experiments acquired at 85 K, the ^{2}H and ^{17}O enhancements are 545 and 115, respectively (Figure 6b and 6c). This makes trityl still one of the most effective radicals to polarize such nuclei.[47,48,84] The EPR spectrum is nearly symmetric which gives rise to the nearly symmetric positive and negative maxima in the DNP field profile. The smaller enhancement for ^{17}O may be attributed to the comparably short polarization build-up time constant (T_B = 5.0 ± 0.6 s) inhibiting saturation. This suggests a relatively fast nuclear relaxation rate that inhibits the build-up of non-Boltzmann polarization. In the case of ^{2}H and ^{13}C,

267 both nuclei exhibit larger DNP gains and both have longer T_B (Table 2). The large quadrupolar
268 coupling of ^{17}O may also be a factor, and studies are currently underway to elucidate this. We
269 would also like to note for all of these nuclei studied the trityl EPR line was not saturated by
270 using 8 W of microwave power, and further enhancement gains should be possible by increasing
271 the available microwave power.

272 **Table 2:** Direct polarization of various biologically relevant nuclei using trityl at 5 T.

Nucleus	ε (positive) (± 10 %)	ε (negative) (± 10 %)	T_B (s)	$\omega_{0I}/2\pi$ (MHz)	Mechanism
$^{1}H^{59}$	90	-81	22	212.03	SE
$^{13}C^{79}$	480	-380	225	53.3	CE/SE
^{2}H	545	-565	75	32.5	CE
$^{17}O^{47}$	115	-116	5.5	28.7	CE

273

274

275

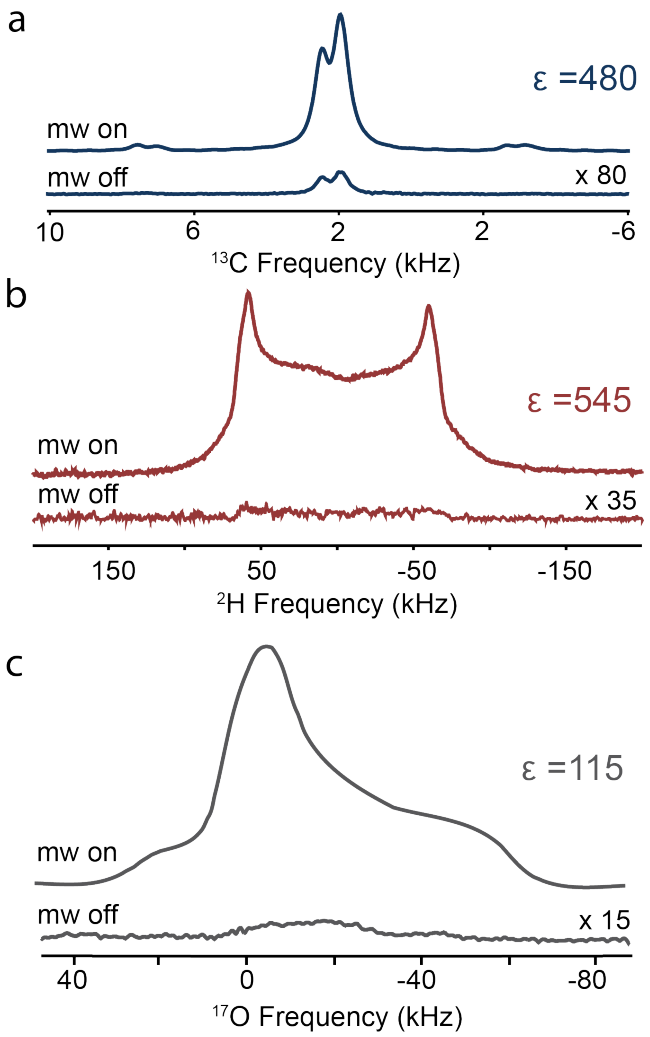

Figure 6: Direct polarization of low-gamma nuclei using 40 mM trityl on (a) ^{13}C (υ_L = 53 MHz), (b) ^{2}H (υ_L = 32 MHz) and (c) ^{17}O (28 MHz) in a glycerol/water cryoprotectant. DNP enhanced signals were acquired using 8 W of CW microwave power with the magnetic field set to the optimum field position (positive) shown in Figure 5.

iii. Sample Preparation Techniques

The effective DNP polarization of a biological solid requires a few key criteria to be met. The first is to disperse the polarizing agent, which allows uniform polarization across the whole sample followed by effective spin-diffusion. For biological samples such as membrane proteins, amyloid fibrils, and peptides, a cryoprotecting matrix such as glycerol/water or DMSO/water,

which forms an amorphous "glassy" state at low temperatures to protect the sample against freezing damage, can be used to homogeneously disperse the polarizing agent for DNP. Labeling of the cryoprotecting matrix, in particular D_2O, deuterated glycerol, and deuterated DMSO, can be used to fine tune ^{1}H-^{1}H spin-diffusion to optimize the obtainable DNP enhancement, while reverse labeling the matrix (e.g., ^{12}C-glycerol) can minimize solvent background. In our experience, a cryoprotecting matrix that is heavily deuterated is optimal for DNP, and typically we prepare our samples in a 60/30/10 v/v d_8-glycerol/D_2O/H_2O. However, the NMR of a homogeneous, amorphous chemical system can be limited in resolution due to line-broadening stemming from a distribution of chemical shift, a commonly observed occurrence for many organic and inorganic amorphous materials, as well as from slower side-chain dynamics at cryogenic temperatures. Despite this limitation, DNP has been successfully applied to heterogeneous systems like the membrane protein bacteriorhodopsin[14,37,38,50,85] and M2[86], and by combining with methods including specific labeling[87-89] and crystal suspension in liquid[39,42,90-92]. DNP NMR also has been demonstrated on various chemical systems without adding a cryoprotectant, due to either thermal stability or self-cryoprotecting ability.[76,93-96]

Figure 7 illustrates the various sample preparation methods both with and without cryoprotecting matrix. Figure 7a and b show DNP of amorphous and crystalline 95% deuterated *ortho*-terphenyl. While both samples show large ^{1}H DNP enhancements, the crystalline sample has somewhat improved resolution of the various ^{13}C resonances. The resolution as described above is not impacted by temperature, but the distribution in chemical shift brought about by the formation of a disordered homogeneous solid. Figure 7c and d show DNP enhanced spectra of apoferritin complex (480 kDa) prepared using either a traditional glycerol/water cryoprotectant (Figure 7c) or the new sedimentation method (SedDNP) (Figure 7d) where free water concentration is significantly reduced either by ultracentrifugation (*ex situ*) or via fast magic

angle spinning (*in situ*).[93,94] Either sedimentation method results in a "microcrystalline" glass that effectively distributes the polarizing agent within the sample, allows efficient spin diffusion through the whole sample, and protects against potential damage from ice crystal formation. Both approaches provide high sensitivity, however the sedimentation method minimizes the solvent present and so reduces the solvent resonances (e.g., glycerol at ~60-70 ppm) while improving the overall filling factor. The sedimentation technique has an added advantage where cooling to cryogenic temperatures and employing DNP can offer additional structural information and constraint not observed at experiments performed at ambient condition. The low temperature spectra can provide extensive information on side chain motion and details concerning aromatic regions that are often lost due to decoupling interference at room temperature.[87,97]

Finally, nanocrystalline preparation of GNNQQNY[90,98] (Figure 7e) by suspension in a cryoprotecting matrix provides high resolution and DNP enhancement for structural understanding in both crystalline and amyloid forms. Wetting of microcrystals have also been attractive for the study of various surface science questions whereby a nitroxide biradical is dispersed into an organic solvent and added to the crystalline material of choice prior to cooling.[42,92,99] Furthermore, a solvent-free dehydration approach whereby the radical is placed onto the system such as glucose or cellulose, followed by evaporation has also recently shown promise for natural abundant systems.[95,96] Although these methods lead to a more heterogeneous distribution of radicals and hence polarization is not uniform within the samples, they maintain excellent sensitivity and produce excellent spectral resolution from an overall smaller effect from paramagnetic broadening.

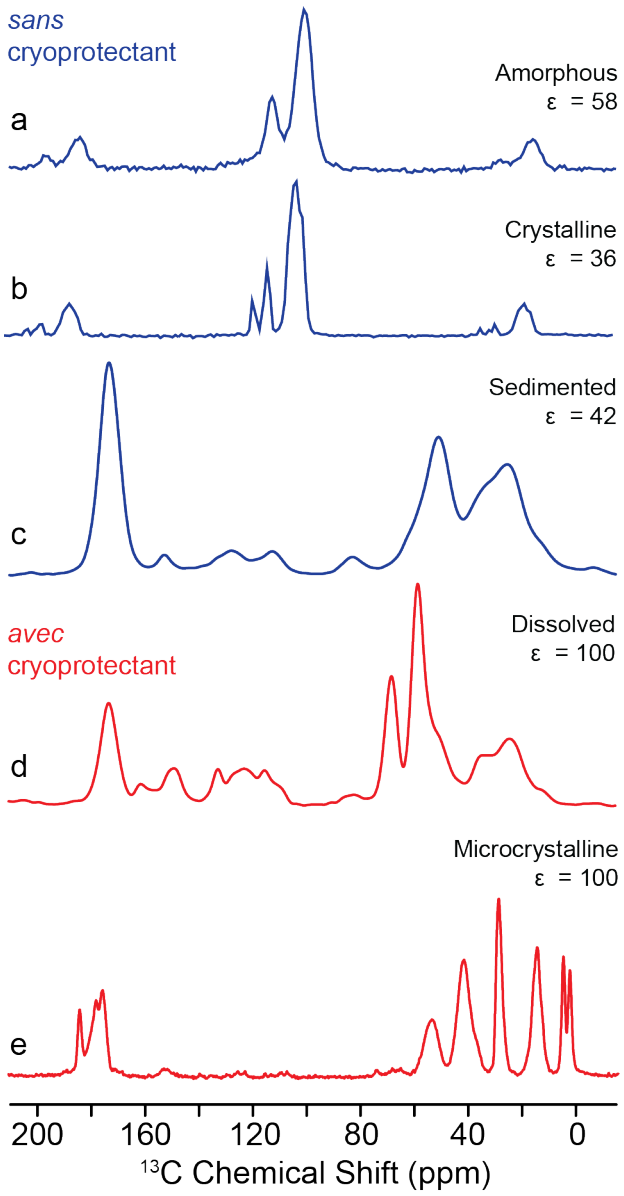

Figure 7: MAS DNP sample preparation protocols for biophysical systems. Without cryoprotecting solvents (*sans*) include distributing a polarizing agent within the organic solid: amorphous (a) or crystalline (b), or using the SedDNP approach (c). Alternative is distributing the radical in a cryoprotecting solvent (*avec*) homogenously (d) or heterogeneously using microcrystals (e).

iv. Improving DNP Instrumentation at High Fields (≥16 T)

In recent years, high-field DNP has evolved beyond 9.4 T (400 MHz, ^{1}H). The innovation in gyrotron technology has led to more adoptions of high-field DNP spectrometers such as the

600 MHz / 395 GHz[53,100] (Osaka University, Japan and University of Warwick, UK), the 700 MHz / 460 GHz[52] (MIT, Cambridge, MA), and the commercial 600 MHz/ 395 GHz and 800 MHz / 527 GHz from Bruker Biospin. However, DNP theory predicts the experiment to be less effective at high fields, with an inverse scaling of CE DNP enhancement with respect to increasing magnetic field.[62] This is because the EPR linewidth of the polarizing agent increases proportionally with respect to the magnetic field ($\Delta \propto B_o$), meaning that the CE matching condition becomes harder to satisfy. The challenge is compounded by the difficult tasks of maintaining effective cooling capabilities at elevated MAS frequencies (e.g., limiting frictional heating) and also coupling gyrotron microwaves to the NMR sample. Therefore, considerable effort has been made to improve instrumentation in order to gain reasonable DNP enhancement at these fields. Given the inherent better resolution of high field NMR (*vide infra*), successful DNP can become a valuable approach to obtain structural information of challenging biological samples.

One particular difficulty in implementing DNP at higher magnetic fields is the transmission of high-power microwaves from the gyrotron to the sample with minimal loss. This can be achieved by using corrugated overmoded waveguides, which are more efficient then the previously used fundamental mode waveguides, to minimize mode conversion and ohmic loss. At the MIT-FBML, the microwave source of the 700 MHz DNP system is a 460 GHz gyrotron operating in the second harmonic, in a $TE_{11,2}$ mode.[101] The produced microwaves are guided through a ~ 465 cm long, 19.05 mm inner diameter (i.d.) corrugated waveguide that connects the 16.4 T NMR magnet and the 8.2 T gyrotron magnet. The alignment is critical to maintain a clean microwave mode with minimum energy loss through the long waveguide, and we were able to achieve less than 1 dB loss from the gyrotron window to the final miter-bend that directs the

364 microwaves into the probe body. The final ~85 cm of the waveguide is located within the NMR
365 probe, and it was initially constructed by a series of down tapers reducing the i.d. from 19.05 to
366 4.6 mm. using a combination of smooth-walled macor, aluminum and copper waveguide portions.
367 However, due to the significant loss of microwave power associated with 4.6 mm waveguide and
368 macor sections at 460 GHz (λ = 0.65 mm), several changes were implemented to improve
369 microwave transmission to the sample. A newly designed waveguide for our home-built DNP
370 NMR probes now includes a modified tapered and corrugated aluminum waveguide section from
371 19.05 to 11.43 mm i.d. at the base of the NMR probe (Figure 8), and at which point the
372 microwaves are directed toward the stator via a 45^{o} miter-bend. The microwaves are then
373 reflected off a copper mirror into a multi-section corrugated waveguide with an 11.43 mm i.d.
374 consists of a stainless steel section at the base which acts as a thermal break followed by two
375 copper sections. The final 50 mm portion approaches the reverse magic-angle microwave beam
376 launcher features an aluminum corrugated part that is tapered from 11.43 to 8 mm i.d. in order to
377 direct and focus the microwave beam into the 3.2 mm MAS stator housing. A small Vespel®
378 washer is installed prior to the final taper to act as an electrical break between the microwaves
379 and the RF. Finally, the waveguide is terminated by a copper microwave launcher at the reverse
380 magic-angle, and aligned using three brass set screws. With these modifications, the new probe
381 waveguide design reduces the loss of microwave power being transmitted to the sample while
382 maintaining the effective Gaussian beam content. The new design has improved the high-field
383 DNP enhancements by 40-50%, from -38 (4) to -53 (5) on a sample of 1 M *^{13}C*-urea at 80 (2) K
384 and from -21 to -33 on a sample of 0.5 M U-^{13}C-proline. Figure 9 shows a DNP enhanced ^{13}C-
385 ^{13}C DARR spectrum of U-^{13}C-proline that illustrates the good resolution and sensitivity gain that
386 can be achieved with high field DNP.
387

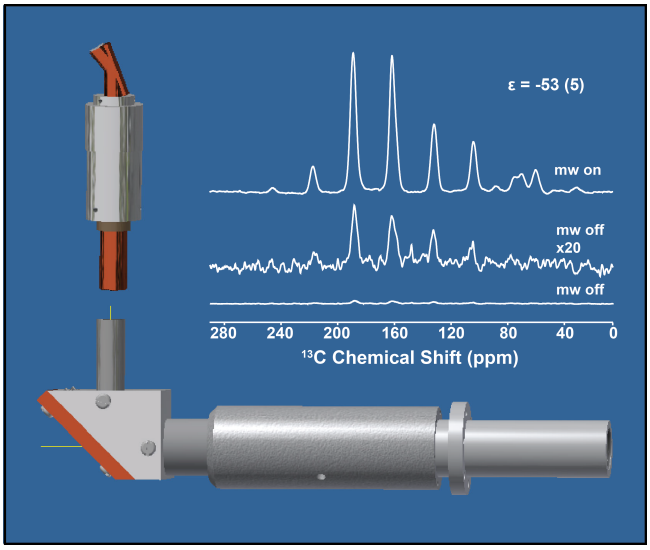

388

389 **Figure 8:** Artistic rendering of the new waveguide designed for the 460 GHz / 700 MHz DNP NMR
390 spectrometer (FBML-MIT). The inset is an $^{13}C^{1}H$ CP on/off spectrum of 1M ^{13}C-Urea in d_8-
391 glycerol/D_2O/H_2O (v/v 60/30/10) with 10 mM TOTAPOL and packed into a 3.2 mm sapphire rotor,
392 acquired at 80 K and a spinning frequency of 5.2 kHz.

393

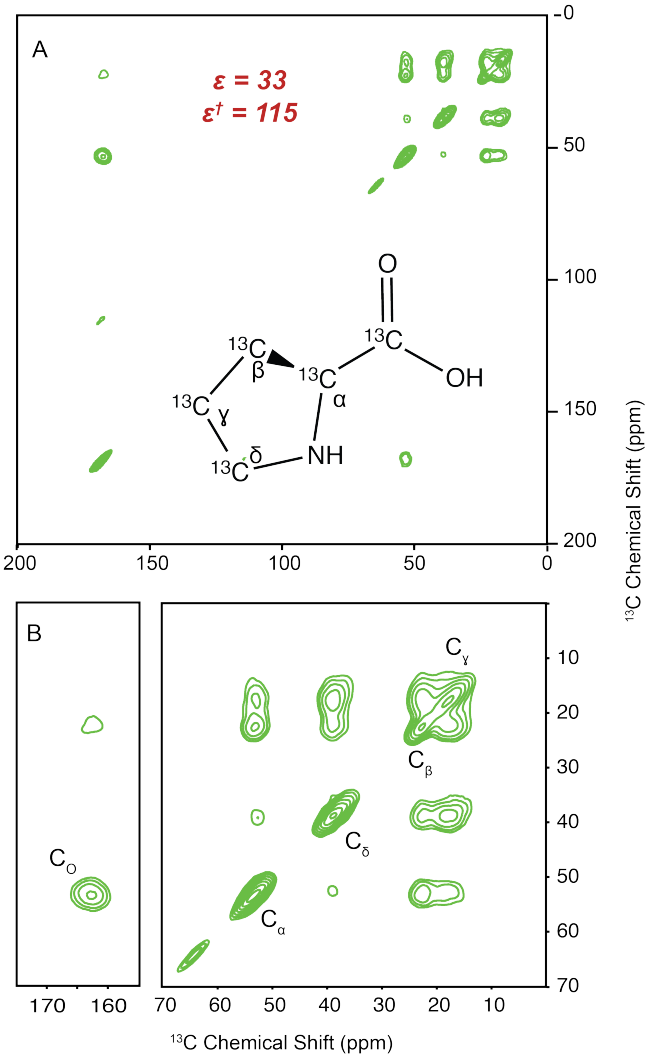

394

395 **Figure 9:** (A) ^{13}C-^{13}C DARR spectrum of U-^{13}C-Proline (0.5 M) in d_8-glycerol/D_2O/H_2O (v/v 60/30/10) with
396 10 mM TOTAPOL (^{1}H enhancement of 33 (3)) using a 20 ms DARR mixing period. (B) An enlarged
397 aliphatic and carbonyl region illustrating the connectivity of U-^{13}C-Proline. Sample was packed into a 3.2
398 mm sapphire rotor, data was acquired with 8 scans, rd = 20 s, 64 increments, 11 W of microwave power,
399 sample temperature 82 (2) K and a spinning frequency of 9,200 Hz.

400

401 We recently used the improved 700 MHz DNP system to study apoferritin, which is an
402 important protein for maintaining available non-toxic soluble forms of iron in various
403 organisms.[102] Apoferritin, the iron-free form, is a 480 kDa globular protein complex consisting

of 24 subunits, with each unit being 20 kDa in size. The protein is a challenging system for NMR due to its large size comprised of nearly 4,000 residues.[103] Nevertheless, chemical shift separation can be achieved at higher magnetic fields, and structural insight can be gained through a combination of approaches including solution and solid-state methods (i.e., SedNMR)[104,105] as well as combining with DNP (i.e., SedDNP).[93] Figure 10 is an overlay of U-^{13}C-apoferritine collected at 212 MHz / 140 GHz and 697 MHz / 460 GHz employing a ^{13}C-^{13}C PDSD dipolar recoupling experiment. Although the DNP enhancement is lower at the higher field (ε = -6, with $\varepsilon^{\dagger}$ = -21 accounting for Boltzmann population difference between cryogenic and room temperature) compares to the lower field enhancement (ε = 42), we can see that the aliphatic region is significantly more dispersed in the higher field spectrum enabling differentiation between the C_{α} and C_{β} region. Continuing effort at improving instrumentation and developing new radicals will potentially increase enhancement further than what is currently obtainable.

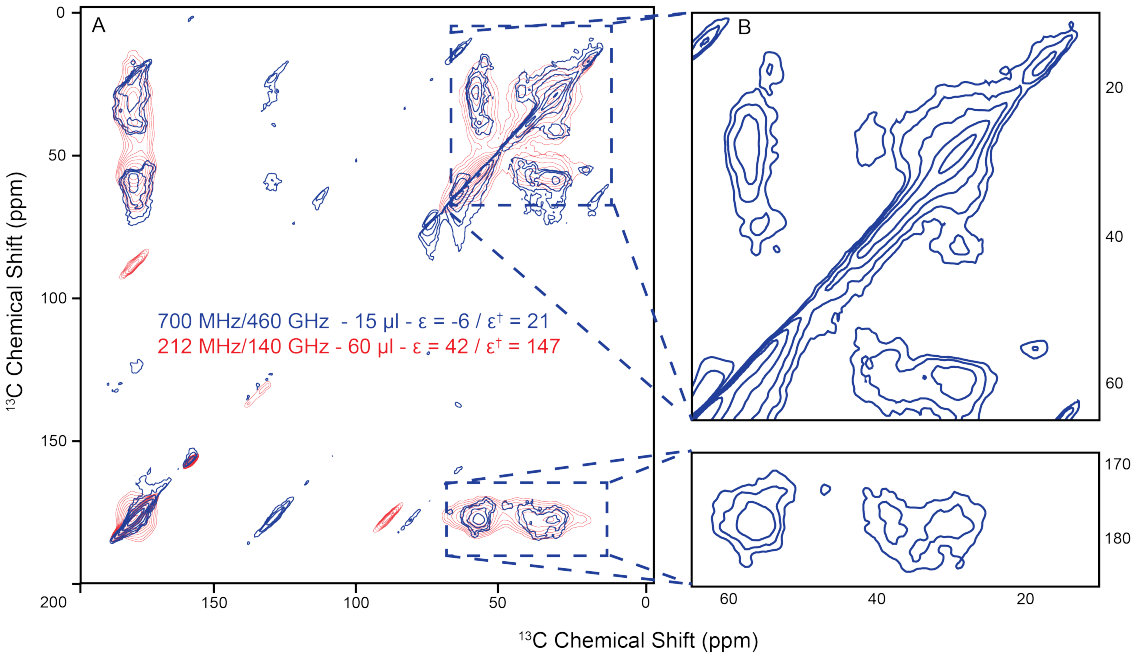

Figure 10: ^{13}C-^{13}C correlation spectrum of U-^{13}C-apoferritin at 5 T (red) and 16.4 T (blue) using DNP MAS NMR.

Conclusion

In this topical review, we discussed the recent DNP efforts at MIT-FBML including new radical polarization-agent development, direct polarization of low-gamma nuclei, various sample preparation methods, and hardware improvements to our 700 MHz / 460 GHz DNP NMR spectrometer. As developmental efforts continue and along with the recent commercialization of DNP systems, we foresee the method achieving greater sensitivity for NMR and becoming a more general method to study various biological and chemical systems. We expect the wider adoption of DNP to be a very fruitful endeavor leading to many new and exciting scientific discoveries.

Acknowledgements

The authors would like to thank Eugenio Daviso, Bjorn Corzilius, Albert Smith, Loren Andreas, Galia Debelouchina, Jennifer Mathies, Michael Colvin, Emilio Nanni, Sudheer Jawla, Ivan Mastrovsky and Richard Temkin for helpful discussions during the course of this research. Ajay Thakkar, Jeffrey Bryant, Ron DeRocher, Michael Mullins, David Ruben and Chris Turner are thanked for technical assistance. The National Institutes of Health through grants EB002804, EB003151, EB002026, EB001960, EB001035, EB001965, and EB004866 supported this research. V.K.M. acknowledges the Natural Science and Engineering Research Council of Canada for a Postdoctoral Fellowship. ‡These authors contributed equally.

References

(1) Harris, R. K. *Journal of Pharmacy and Pharmacology* **2007**, *59*, 225.
(2) Vogt, F. G. *Future Medicinal Chemistry* **2010**, *2*, 915.
(3) Brown, S. P. *Solid State Nuclear Magnetic Resonance* **2012**, *41*, 1.
(4) McDermott, A. *Annual Review of Biophysics* **2009**, *38*, 385.
(5) Andreas, L. B.; Eddy, M. T.; Pielak, R. M.; Chou, J.; Griffin, R. G. *Journal of the American Chemical Society* **2010**, *132*, 10958.
(6) Cady, S.; Wang, T.; Hong, M. *Journal of the American Chemical Society* **2011**, *133*, 11572.
(7) Eddy, M. T.; Ong, T. C.; Clark, L.; Teijido, O.; van der Wel, P. C. A.; Garces, R.; Wagner, G.; Rostovtseva, T. K.; Griffin, R. G. *Journal of the American Chemical Society* **2012**, *134*, 6375.
(8) Shi, L. C.; Ahmed, M. A. M.; Zhang, W. R.; Whited, G.; Brown, L. S.; Ladizhansky, V. *Journal of Molecular Biology* **2009**, *386*, 1078.
(9) Tycko, R. *Protein and Peptide Letters* **2006**, *13*, 229.
(10) Bayro, M. J.; Debelouchina, G. T.; Eddy, M. T.; Birkett, N. R.; MacPhee, C. E.; Rosay, M.; Maas, W. E.; Dobson, C. M.; Griffin, R. G. *Journal of the American Chemical Society* **2011**, *133*, 13967.
(11) Fitzpatrick, A. W. P.; Debelouchina, G. T.; Bayro, M. J.; Clare, D. K.; Caporini, M. A.; Bajaj, V. S.; Jaroniec, C. P.; Wang, L. C.; Ladizhansky, V.; Muller, S. A.; MacPhee, C. E.; Waudby, C. A.; Mott, H. R.; De Simone, A.; Knowles, T. P. J.; Saibil, H. R.; Vendruscolo, M.; Orlova, E. V.; Griffin, R. G.; Dobson, C. M. *Proceedings of the National Academy of Sciences of the United States of America* **2013**, *110*, 5468.
(12) Bertini, I.; Gonnelli, L.; Luchinat, C.; Mao, J. F.; Nesi, A. *Journal of the American Chemical Society* **2011**, *133*, 16013.
(13) Bertini, I.; Gallo, G.; Korsak, M.; Luchinat, C.; Mao, J.; Ravera, E. *ChemBioChem* **2013**, n/a.
(14) Ni, Q. Z.; Daviso, E.; Cana, T. V.; Markhasin, E.; Jawla, S. K.; Temkin, R. J.; Herzfeld, J.; Griffin, R. G. *Accounts of Chem Research* **2013**, *(in press)*.
(15) Maly, T.; Debelouchina, G. T.; Bajaj, V. S.; Hu, K. N.; Joo, C. G.; Mak-Jurkauskas, M. L.; Sirigiri, J. R.; van der Wel, P. C. A.; Herzfeld, J.; Temkin, R. J.; Griffin, R. G. *Journal of Chemical Physics* **2008**, *128*.
(16) Abragam, A.; Goldman, M. *Nuclear Magnetism: Order and Disorder*; Clarendon Press: Oxford, 1982.
(17) Atsarkin, V. A. *Soviet Physics Solid State* **1978**, *21*, 725.
(18) Wind, R. A.; Duijvestijn, M. J.; Vanderlugt, C.; Manenschijn, A.; Vriend, J. *Progress in Nuclear Magnetic Resonance Spectroscopy* **1985**, *17*, 33.
(19) Barnes, A. B.; Paëpe, G. D.; Wel, P. C. A. v. d.; Hu, K.-N.; Joo, C.-G.; Bajaj, V. S.; Mak-Jurkauskas, M. L.; Sirigiri, J. R.; Herzfeld, J.; Temkin, R. J.; Griffin, R. G. *Applied Magnetic Resonance* **2008**, *34*, 237.
(20) Rossini, A. J.; Zagdoun, A.; Lelli, M.; Lesage, A.; Copéret, C.; Emsley, L. *Accounts of Chemical Research* **2013**.
(21) Overhauser, A. W. *Physical Review* **1953**, *92*, 411.
(22) Carver, T. R.; Slichter, C. P. *Physical Review* **1953**, *92*, 212.
(23) Jeffries, C. D. *Physical Review* **1957**, *106*, 164.

(24) Abragam, A.; Proctor, W. G. *Comptes Rendus Hebdomadaires Des Seances De L Academie Des Sciences* **1958**, *246*, 2253.
(25) Jeffries, C. D. *Physical Review* **1960**, *117*, 1056.
(26) Kessenikh, A. V.; Lushchikov, V. I.; Manenkov, A. A.; Taran, Y. V. *Soviet Physics-Solid State* **1963**, *5*, 321.
(27) Kessenikh, A. V.; Manenkov, A. A.; Pyatnitskii, G. I. *Soviet Physics-Solid State* **1964**, *6*, 641.
(28) Hwang, C. F.; Hill, D. A. *Physical Review Letters* **1967**, *18*, 110.
(29) Hwang, C. F.; Hill, D. A. *Physical Review Letters* **1967**, *19*, 1011.
(30) Wollan, D. S. *Physical Review B* **1976**, *13*, 3671.
(31) Goldman, M. *Spin temperature and nuclear magnetic resonance in solids*; Clarendon Press: Oxford,, 1970.
(32) Duijvestijn, M. J.; Wind, R. A.; Smidt, J. *Physica B & C* **1986**, *138*, 147.
(33) Wenckebach, W. T.; Swanenburg, T. J. B.; Poulis, N. J. *Physics Reports* **1974**, *14*, 181.
(34) Afeworki, M.; McKay, R. A.; Schaefer, J. *Macromolecules* **1992**, *25*, 4048.
(35) Afeworki, M.; Vega, S.; Schaefer, J. *Macromolecules* **1992**, *25*, 4100.
(36) Becerra, L. R.; Gerfen, G. J.; Bellew, B. F.; Bryant, J. A.; Hall, D. A.; Inati, S. J.; Weber, R. T.; Un, S.; Prisner, T. F.; Mcdermott, A. E.; Fishbein, K. W.; Kreischer, K. E.; Temkin, R. J.; Singel, D. J.; Griffin, R. G. *Journal of Magnetic Resonance Series A* **1995**, *117*, 28.
(37) Mak-Jurkauskas, M. L.; Bajaj, V. S.; Hornstein, M. K.; Belenky, M.; Griffin, R. G.; Herzfeld, J. *Proceedings of the National Academy of Sciences of the United States of America* **2008**, *105*, 883.
(38) Bajaj, V. S.; Mak-Jurkauskas, M. L.; Belenky, M.; Herzfeld, J.; Griffin, R. G. *Proceedings of the National Academy of Sciences of the United States of America* **2009**, *106*, 9244.
(39) Debelouchina, G. T.; Bayro, M. J.; van der Wel, P. C. A.; Caporini, M. A.; Barnes, A. B.; Rosay, M.; Maas, W. E.; Griffin, R. G. *Physical Chemistry Chemical Physics* **2010**, *12*, 5911.
(40) Akbey, Ü.; Franks, W. T.; Linden, A.; Lange, S.; Griffin, R. G.; Rossum, B.-J. v.; Oschkinat, H. *Angewandte Chemie International Edition* **2010**, *49*, 7803.
(41) Linden, A. H.; Lange, S.; Franks, W. T.; Akbey, U.; Specker, E.; Rossum, B. J. v.; Oschkinat, H. *J. Amer. Chem. Soc.* **2011**, *133*, 19266.
(42) Lesage, A.; Lelli, M.; Gajan, D.; Caporini, M. A.; Vitzthum, V.; Mieville, P.; Alauzun, J.; Roussey, A.; Thieuleux, C.; Mehdi, A.; Bodenhausen, G.; Coperet, C.; Emsley, L. *J Am Chem Soc* **2010**, *132*, 15459.
(43) Lumata, L.; Merritt, M. E.; Hashami, Z.; Ratnakar, S. J.; Kovacs, Z. *Angewandte Chemie-International Edition* **2012**, *51*, 525.
(44) Michaelis, V. K.; Markhasin, E.; Daviso, E.; Herzfeld, J.; Griffin, R. G. *Journal of Physical Chemistry Letters* **2012**, *3*, 2030.
(45) Vitzthum, V.; Mieville, P.; Carnevale, D.; Caporini, M. A.; Gajan, D.; Cope, C.; Lelli, M.; Zagdoun, A.; Rossini, A. J.; Lesage, A.; Emsley, L.; Bodenhausen, G. *Chem. Commun.* **2012**, *48*, 1988.
(46) Vitzthum, V.; Caporini, M. A.; Bodenhausen, G. *Jour Magn Resonance* **2010**, *204*.
(47) Michaelis, V. K.; Corzilius, B.; Smith, A. A.; Griffin, R. G. *Submitted* **2013**.
(48) Maly, T.; Andreas, L. B.; Smith, A. A.; Griffin, R. G. *Physical Chemistry Chemical Physics* **2010**, *12*, 5872.

(49) Blanc, F.; Sperrin, L.; Jefferson, D. A.; Pawsey, S.; Rosay, M.; Grey, C. P. *J Am Chem Soc* **2013**, *135*, 2975.
(50) Bajaj, V. S.; Hornstein, M. K.; Kreischer, K. E.; Sirigiri, J. R.; Woskov, P. P.; Mak-Jurkauskas, M. L.; Herzfeld, J.; Temkin, R. J.; Griffin, R. G. *Journal of Magnetic Resonance* **2007**, *189*, 251.
(51) Allen, P. J.; Creuzet, F.; Degroot, H. J. M.; Griffin, R. G. *Journal of Magnetic Resonance* **1991**, *92*, 614.
(52) Barnes, A. B.; Markhasin, E.; Daviso, E.; Michaelis, V. K.; Nanni, E. A.; Jawla, S. K.; Mena, E. L.; DeRocher, R.; Thakkar, A.; Woskov, P. P.; Herzfeld, J.; Temkin, R. J.; Griffin, R. G. *Journal of Magnetic Resonance* **2012**, *224*, 1.
(53) Matsuki, Y.; Takahashi, H.; Ueda, K.; Idehara, T.; Ogawa, I.; Toda, M.; Akutsu, H.; Fujiwara, T. *Physical Chemistry Chemical Physics* **2010**, *12*, 5799.
(54) Barnes, A. B.; Mak-Jurkauskas, M. L.; Matsuki, Y.; Bajaj, V. S.; van der Wel, P. C. A.; DeRocher, R.; Bryant, J.; Sirigiri, J. R.; Temkin, R. J.; Lugtenburg, J.; Herzfeld, J.; Griffin, R. G. *Journal of Magnetic Resonance* **2009**, *198*, 261.
(55) Shimon, D.; Hovav, Y.; Feintuch, A.; Goldfarb, D.; Vega, S. *Physical Chemistry Chemical Physics* **2012**, *14*, 5729.
(56) Hovav, Y.; Levinkron, O.; Feintuch, A.; Vega, S. *Applied Magnetic Resonance* **2012**, *43*, 21.
(57) Hu, K. N.; Bajaj, V. S.; Rosay, M.; Griffin, R. G. *Journal of Chemical Physics* **2007**, *126*.
(58) Corzilius, B.; Smith, A. A.; Barnes, A. B.; Luchinat, C.; Bertini, I.; Griffin, R. G. *J Am Chem Soc* **2011**, *133*, 5648.
(59) Corzilius, B.; Smith, A. A.; Griffin, R. G. *Journal of Chemical Physics* **2012**, *137*.
(60) Smith, A. A.; Corzilius, B.; Barnes, A. B.; Maly, T.; Griffin, R. G. *Journal of Chemical Physics* **2012**, *136*.
(61) Smith, A. A.; Corzilius, B.; Bryant, J. A.; DeRocher, R.; Woskov, P. P.; Temkin, R. J.; Griffin, R. G. *Journal of Magnetic Resonance* **2012**, *223*, 170.
(62) Hu, K. N.; Debelouchina, G. T.; Smith, A. A.; Griffin, R. G. *Journal of Chemical Physics* **2011**, *134*.
(63) Hovav, Y.; Feintuch, A.; Vega, S. *Journal of magnetic resonance* **2012**, *214*, 29.
(64) Hu, K.-N.; Song, C.; Yu, H.-h.; Swager, T. M.; Griffin, R. G. *J. Chem. Phys.* **2008**, *128*, 052321.
(65) Thurber, K. R.; Tycko, R. *The Journal of Chemical Physics* **2012**, *137*.
(66) Mentink-Vigier, F.; Akbey, Ü.; Hovav, Y.; Vega, S.; Oschkinat, H.; Feintuch, A. *Journal of magnetic resonance* **2012**, *224*, 13.
(67) Gerfen, G. J.; Becerra, L. R.; Hall, D. A.; Griffin, R. G.; Temkin, R. J.; Singel, D. J. *Journal of Chemical Physics* **1995**, *102*, 9494.
(68) Hall, D. A.; Maus, D. C.; Gerfen, G. J.; Inati, S. J.; Becerra, L. R.; Dahlquist, F. W.; Griffin, R. G. *Science* **1997**, *276*, 930.
(69) Song, C. S.; Hu, K. N.; Joo, C. G.; Swager, T. M.; Griffin, R. G. *J Am Chem Soc* **2006**, *128*, 11385.
(70) Matsuki, Y.; Maly, T.; Ouari, O.; Karoui, H.; Le Moigne, F.; Rizzato, E.; Lyubenova, S.; Herzfeld, J.; Prisner, T.; Tordo, P.; Griffin, R. G. *Angewandte Chemie-International Edition* **2009**, *48*, 4996.
(71) Kiesewetter, M. K.; Corzilius, B.; Smith, A. A.; Griffin, R. G.; Swager, T. M. *J Am Chem Soc* **2012**, *134*, 4537.

(72) Zagdoun, A.; Casano, G.; Ouari, O.; Lapadula, G.; Rossini, A. J.; Lelli, M.; Baffert, M.; Gajan, D.; Veyre, L.; Maas, W. E.; Rosay, M.; Weber, R. T.; Thieuleux, C.; Coperet, C.; Lesage, A.; Tordo, P.; Emsley, L. *J Am Chem Soc* **2012**, *134*, 2284.

(73) Zagdoun, A.; Casano, G.; Ouari, O.; Schwarzwälder, M.; Rossini, A. J.; Aussenac, F.; Yulikov, M.; Jeschke, G.; Copéret, C.; Lesage, A.; Tordo, P.; Emsley, L. *J Am Chem Soc* **2013**.

(74) Borka, L. *Acta Pharmaceutica Suecica* **1974**, *11*, 295.

(75) Imaizumi, H.; Nambu, N.; Nagai, T. *Chemical & Pharmaceutical Bulletin* **1980**, *28*, 2565.

(76) Ong, T. C.; Mak-Jurkauskas, M. L.; Walish, J. J.; Michaelis, V. K.; Corzilius, B.; Smith, A. A.; Clausen, A. M.; Cheetham, J. C.; Swager, T. M.; Griffin, R. G. *Journal of Physical Chemistry B* **2013**, *117*, 3040.

(77) Frantz, D. K.; Walish, J. J.; Swager, T. M. *Organic Letters* **2013**.

(78) Haze, O.; Corzilius, B.; Smith, A. A.; Griffin, R. G.; Swager, T. M. *J. Am. Chem. Soc.* **2012**, *134*, 14287.

(79) Michaelis, V. K.; Smith, A. A.; Corzilius, B.; Haze, O.; Swager, T. M.; Griffin, R. G. *J. Am. Chem. Soc.* **2013**, *In press*.

(80) Ardenkjaer-Larsen, J. H.; Macholl, S.; Johannesson, H. *Applied Magnetic Resonance* **2008**, *34*, 509.

(81) Thaning, M.; Nycomed Imaging AS: USA, 2000; Vol. 06013810.

(82) Farrar, C. T.; Hall, D. A.; Gerfen, G. J.; Rosay, M.; Ardenkjaer-Larsen, J. H.; Griffin, R. G. *Journal of Magnetic Resonance* **2000**, *144*, 134.

(83) Maly, T.; Miller, A.-F.; Griffin, R. G. *Chemphyschem* **2010**, *11*, 999.

(84) Michaelis, V. K.; Markhasin, E.; Daviso, E.; Corzilius, B.; Smith, A.; Herzfeld, J.; Griffin, R. G. In *Experimental NMR Conference* Miami, FL, 2012.

(85) Barnes, A. B.; Corzilius, B.; Mak-Jurkauskas, M. L.; Andreas, L. B.; Bajaj, V. S.; Matsuki, Y.; Belenky, M. L.; Lugtenburg, J.; Sirigiri, J. R.; Temkin, R. J.; Herzfeld, J.; Griffin, R. G. *Phys. Chem. Chem. Phys.* **2010**, *12*.

(86) Andreas, L. B.; Barnes, A. B.; Corzilius, B.; Chou, J. J.; Miller, E. A.; Caporini, M.; Rosay, M.; Griffin, R. G. *Biochemistry* **2013**, *52*, 2774−2782.

(87) Bayro, M. J.; Debelouchina, G. T.; Eddy, M. T.; Birkett, N. R.; MacPhee, C. E.; Rosay, M.; Maas, W. E.; Dobson, C. M.; Griffin, R. G. *J. Am. Chem. Soc.* **2011**, *133*, 13967.

(88) Bayro, M. J.; Maly, T.; Birkett, N.; MacPhee, C.; Dobson, C. M.; Griffin, R. G. *Biochemistry* **2010**, *49*, 7474.

(89) Debelouchina, G. T.; Platt, G. W.; Bayro, M. J.; Radford, S. E.; Griffin, R. G. *J. Am. Chem. Soc.* **2010**, *132*, 17077.

(90) van der Wel, P. C. A.; Hu, K. N.; Lewandowski, J.; Griffin, R. G. *J Am Chem Soc* **2006**, *128*, 10840.

(91) Rossini, A. J.; Zagdoun, A.; Hegner, F.; Schwarzwälder, M.; Gajan, D.; Copéret, C.; Lesage, A.; Emsley, L. *J. Amer. Chem. Soc.* **2012**, *134*, 16899−16908.

(92) Lelli, M.; Gajan, D.; Lesage, A.; Caporini, M. A.; Vitzthum, V.; Mieville, P.; Heroguel, F.; Rascon, F.; Roussey, A.; Thieuleux, C.; Boualleg, M.; Veyre, L.; Bodenhausen, G.; Coperet, C.; Emsley, L. *J. Am. Chem. Soc.* **2011**, *133*, 2104.

(93) Ravera, E.; Corzilius, B.; Michaelis, V. K.; Rosa, C.; Griffin, R. G.; Luchinat, C.; Bertini, I. *J. Am. Chem. Soc.* **2013**, *(in press)*.

(94) Ravera, E.; Corzilius, B.; Michaelis, V. K.; Luchinat, C.; Griffin, R. G.; Bertini, I. *Journal of Physical Chemistry B* **2013**, *submitted for publication*.

(95) Takahashi, H.; Ayala, I.; Bardet, M.; De Paëpe, G.; Simorre, J.-P.; Hediger, S. *J Am Chem Soc* **2013**, *135*, 5105.
(96) Takahashi, H.; Hediger, S.; De Paepe, G. *Chemical Communications* **2013**.
(97) Bajaj, V. S.; Wel, P. C. A. v. d.; Griffin, R. G. *Jour. Amer. Chem. Soc* **2009**, *131*, 118.
(98) Debelouchina, G. T.; Bayro, M. J.; Wel, P. C. A. v. d.; Caporini, M. A.; Barnes, A. B.; Rosay, M.; Maas, W. E.; Griffin, R. G. *Phys. Chem. Chem. Phys.* **2010**, *12*.
(99) Lafon, O.; Thankamony, A. S. L.; Kobayashi, T.; Carnevale, D.; Vitzthum, V.; Slowing, I. I.; Kandel, K.; Vezin, H.; Amoureux, J.-P.; Bodenhausen, G.; Pruski, M. *The Journal of Physical Chemistry C* **2012**, *117*, 1375.
(100) Pike, K. J.; Kemp, T. F.; Takahashi, H.; Day, R.; Howes, A. P.; Kryukov, E. V.; MacDonald, J. F.; Collis, A. E.; Bolton, D. R.; Wylde, R. J.; Orwick, M.; Kosuga, K.; Clark, A. J.; Idehara, T.; Watts, A.; Smith, G. M.; Newton, M. E.; Dupree, R.; Smith, M. E. *Journal of magnetic resonance* **2012**, *215*, 1.
(101) Torrezan, A. C.; Han, S.-T.; Mastovsky, I.; Shapiro, M. A.; Sirigiri, J. R.; Temkin, R. J.; Barnes, A. B.; Griffin, R. G. *IEEE Transactions on Plasma Science* **2010**, *38*, 1150.
(102) Theil, E. C. *Annual Review of Biochemistry* **1987**, *56*, 289.
(103) Harrison, P. M.; Mainwaring, W. I.; Hofmann, T. *Journal of Molecular Biology* **1962**, *4*, 251.
(104) Bertini, I.; Engelke, F.; Luchinat, C.; Parigi, G.; Ravera, E.; Rosa, C.; Turano, P. *Physical Chemistry Chemical Physics* **2012**, *14*, 439.
(105) Bertini, I.; Luchinat, C.; Parigi, G.; Ravera, E.; Reif, B.; Turano, P. *Proc. Natl. Acad. Sci. U. S. A.* **2011**, *108*, 10396.